

## LETTERS

The purpose of this Letters section is to provide rapid dissemination of important new results in the fields regularly covered by *Physics of Fluids*. Results of extended research should not be presented as a series of letters in place of comprehensive articles. Letters cannot exceed four printed pages in length, including space allowed for title, figures, tables, references and an abstract limited to about 100 words. There is a three-month time limit, from date of receipt to acceptance, for processing Letter manuscripts. Authors must also submit a brief statement justifying rapid publication in the Letters section.

## Symmetry breaking to a rotating wave in a lid-driven cylinder with a free surface: Experimental observation

A. H. Hirsaa<sup>a)</sup>

Department of Mechanical, Aerospace, and Nuclear Engineering, Rensselaer Polytechnic Institute, Troy, New York 12180-3590

J. M. Lopez<sup>b)</sup>

Department of Mathematics and Statistics, Arizona State University, Tempe, Arizona 85287-1804

R. Miraghaie

Department of Mechanical, Aerospace, and Nuclear Engineering, Rensselaer Polytechnic Institute, Troy, New York 12180-3590

(Received 9 January 2002; accepted 27 February 2002; published 16 April 2002)

A systematic experimental investigation of the flow in an open cylinder, driven by the constant rotation of the bottom endwall, shows that axisymmetry is spontaneously broken via a supercritical Hopf bifurcation to a rotating wave with azimuthal wave number 4. The physical mechanism responsible for the symmetry breaking is shown to be due to the instability of the shear layer that is produced by the boundary layer on the bottom rotating endwall being turned into the interior by the stationary sidewall. Comparison with other experiments and numerical studies (restricted to axisymmetric subspaces) sheds new light on disparate observations in the literature and helps distinguish between spontaneous and forced (via imperfections) symmetry breaking. © 2002 American Institute of Physics. [DOI: 10.1063/1.1471912]

There is much interest in the stability of rotating shear flows in a wide range of circumstances, from industrial machinery flows to geophysical and astrophysical flows, and from fundamental perspectives. A primary mode of instability of rotating shear flows is a symmetry breaking bifurcation to rotating waves. A canonical flow in which to study rotating shear flow and examine such phenomena as rotating waves is the lid-driven flow in a stationary cylinder. Although several studies have appeared in the literature, the question of how azimuthal symmetry is broken has not yet been fully addressed. Much progress has recently been made for the case where the top of the cylinder is a no-slip wall.<sup>1–6</sup> Only a few experimental studies have appeared investigating the flow with a free surface top,<sup>7–9</sup> and none of these have clarified how symmetry is broken. All of the numerical work on the free surface problem has been restricted to axisymmetric flow.<sup>10–13</sup>

Experiments in the free surface case are complicated, compared to the no-slip top case, by several factors, including surface contamination (especially in the case of water), gas–liquid–solid contact angle other than 90°, and misalignment of the cylinder axis and gravity. These complications

are in addition to the susceptibility of the base flow to geometric imperfections, including out of roundness of the cylinder and misalignment of the cylinder axis and the floor's center of rotation. Even a slight misalignment of an essentially perfect cylinder's axis and floor center of rotation can result in a nonaxisymmetric flow (azimuthal mode  $k=1$  wave), observed in any azimuthal plane through the cylinder. Such misalignments lead to *forced* symmetry breaking. In the present study, we found that if a (precision bore) cylinder is misaligned by as little as 0.01 cm (or  $2 \times 10^{-3}$  times the cylinder diameter), the rotating wave which results from *spontaneous* symmetry breaking was not observed, even at a Re several hundred larger than the onset of the instability for a well-aligned case. This is one of the fundamental issues we aim to address in this Letter.

The flow in the stationary cylinder of aspect ratio  $H/R$  with a floor rotating at  $\Omega$  rad/s and a free surface was studied using the apparatus depicted in Fig. 1. The floor consisted of an optical-quality window (BK-7 glass, flat to within  $\pm 0.0025$  cm) which was held by a 20.32 cm ID, precision ball bearing (Applied Industrial Technologies, model KD080XPO). The optical window was mounted in the ball bearing using a retaining cylinder with a compliant silicone sealant, and three fine-pitch alignment screws were utilized to make the rotation plane of the window true to within  $\pm 0.001$  cm (at  $R$ ). The bearing was press-fitted into a 2.5 cm

<sup>a)</sup>Electronic mail: hirsaa@rpi.edu

<sup>b)</sup>Electronic mail: lopez@math.asu.edu

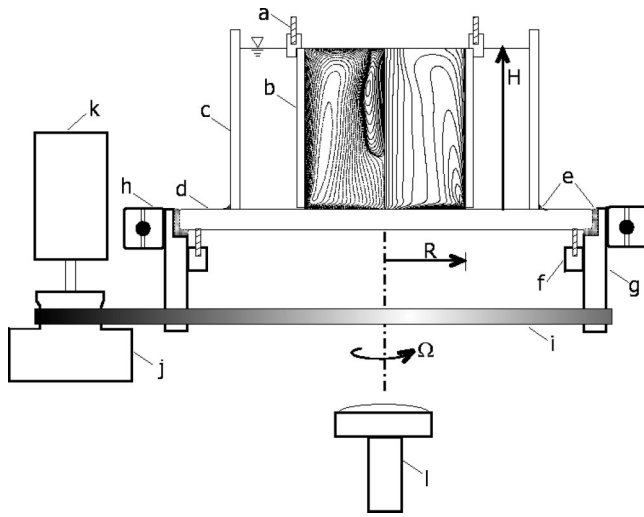


FIG. 1. Schematic of the flow apparatus; inset shows computed streamlines (left meridional half plane) and vortex lines (right meridional half plane) of the steady axisymmetric basic state at  $Re=1900$  and  $H/R=2$ . The letters indicate: stationary cylinder retainer ring and alignment screws (a), stationary cylinder (b), water container cylinder (c); rotating floor (d), silicone sealant (e), rotating floor alignment screws (f), rotating floor retainer and belt pulley (g), ball bearing (h), drive belt (i), motor pulley and flywheel (j), stepper motor (k), and DPIV camera (l).

thick Lexan plate, mounted on an optical table. Several lead bricks (460 Newtons total) were attached to the Lexan plate to dampen any vibrations. The floor was rotated via a drive belt and a computer-operated stepper motor fitted with a 10 cm diameter, 5 cm long brass flywheel. The combination of the drive belt, flywheel and micro-stepping (typically about 41000 microsteps per revolution of floor), made the rotation of the floor relatively free from vibrations. The cylinder was made of precision bore glass (Ace Glass, Trubore) with inner diameter of  $5.000 \pm 0.001$  cm cut to a height of  $5.00 \pm 0.01$  cm. The cylinder was lightly press-fitted into a one-piece retainer, machined from Plexiglas, that contacted the cylinder at three points to minimize optical blockage. The retainer was held by three fine-pitch screws onto the cover plate, allowing the cylinder to be made perpendicular to the rotating floor. The cylinder was centered to within 0.004 cm of the optical floor's center of rotation, using alignment screws on the cover plate. The gap between the cylinder bottom and the rotating floor was set to  $0.006 \pm 0.001$  cm. The top rim of the cylinder was coated with a thin paraffin film to allow the contact line to be pinned. Thus, by filling the system up to the rim, a flat interface (to within  $\pm 0.002$  cm) could be obtained. The paraffin coating did not contaminate the water in the system. The water in the system was contained by a glass cylinder (nominal ID of 11.1 cm, wall thickness of 0.3 cm, and height of 5.6 cm) with its grounded bottom cemented from the outside to the rotating floor. The system was filled with double-distilled water (at  $22^\circ\text{C}$ , where the kinematic viscosity  $\nu=0.00957$   $\text{cm}^2/\text{s}$ ), seeded with 21 micron polystyrene particles (Duke Scientific, 7520A) for the digital particle image velocimetry (DPIV) measurements. The procedure described in Ref. 14 was followed for cleaning the particles. The purity of the surface of the seeded water was checked by surface tension measurements during rapid compression in a Langmuir

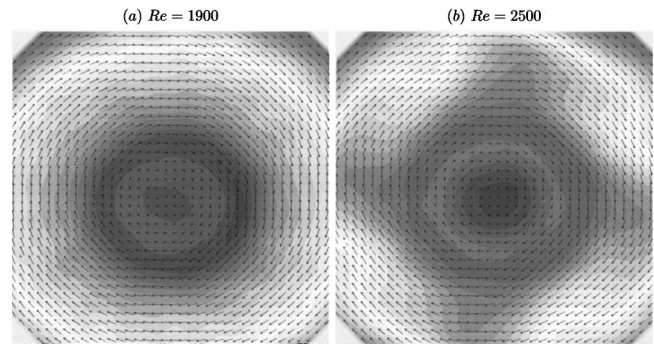


FIG. 2. Axial vorticity (contours) and horizontal velocity (arrows), measured via DPIV, at height  $0.76H$ , for (a) a steady axisymmetric basic state at  $Re=1900$ , and (b) a  $k=4$  rotating wave state at  $Re=2500$ . The noise in the data was reduced by phase averaging at  $1/4$  rotation.

trough. The details of the DPIV system can also be found in Ref. 14.

In the absence of imperfections, the system is  $SO(2)$  invariant, i.e., invariant to arbitrary rotations about the axis, and with the experimental apparatus, we have taken much care to minimize imperfections. As such, the basic flow state is also  $SO(2)$  invariant, i.e., axisymmetric and steady. The meridional structure (i.e., in the  $r$  and  $z$  directions) of the basic state, however, is not trivial. It consists of a boundary layer on the rotating bottom disk that is turned into the interior by the stationary cylinder sidewall, forming a shear layer that has a jet-like velocity profile into the azimuthal direction. In Fig. 1, the streamlines (left) and vortex lines (right) projected onto the meridional plane for a basic state at  $Re = \Omega R^2/\nu = 1900$  and  $H/R = 2$  are shown; the structure of the shear layer is apparent. This basic state was computed with an axisymmetric code, described in detail in Ref. 11. The flow has an overturning nature in the meridional plane, as well as a recirculation zone at the axis, as is characteristic of these swirling flows due to centrifugal effects associated with the overturning flow attempting to bring high angular momentum fluid in towards the axis. In this example, the flow stagnates on the free surface to form the recirculation. At lower  $Re$ , it tends to stagnate on the axis. Detailed accounts of the changes in the structure of the basic state with parameter variation are presented in Refs. 11 and 13. In this Letter, we address the instability of the basic state. We demonstrate experimentally that for  $H/R = 2$ , instability is due to a supercritical symmetry breaking Hopf bifurcation leading to a rotating wave state with azimuthal wave number  $k=4$ , and that the instability is of the shear layer.

Figure 2 shows the axial vorticity and horizontal velocity at a height of  $0.76H$  measured using DPIV. A horizontal laser light sheet of 0.1 cm (or  $0.02H$ ) thickness was utilized in this measurement. Figure 2(a) shows that at  $Re=1900$  the flow is essentially axisymmetric, including the structure of the recirculation zone in the center (see the computed streamlines in the meridional plane shown on the left meridional half plane in Fig. 1). The inner radius of the annular region with large axial vorticity (clockwise rotation, as viewed from below by the DPIV camera) delineates the recirculation region. The boundary layer on the cylinder (negative axial vorticity) is clearly visible in the four corners of each plot. The slightly

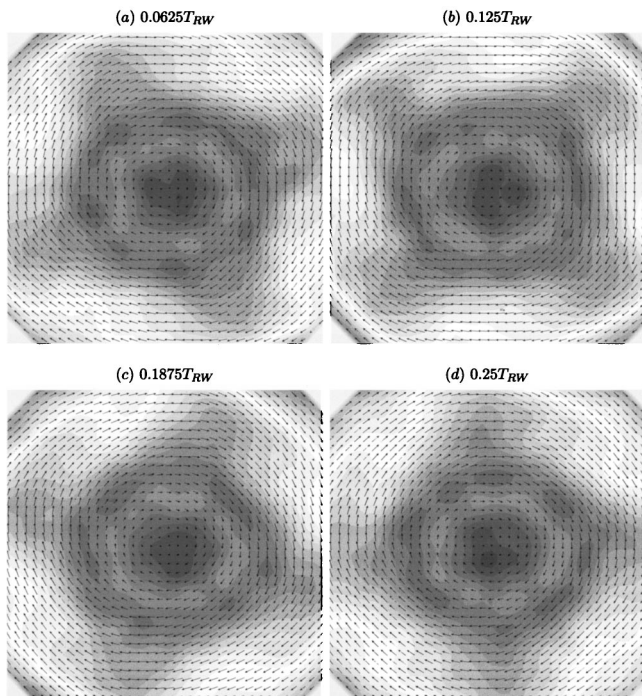


FIG. 3. Four snapshots of the axial vorticity and horizontal velocity at height  $z=0.76H$  of the  $k=4$  rotating wave at  $Re=2500$ , at four equally spaced phases over a quarter rotation of the wave.

wavy pattern in some of the vorticity contours in Fig. 2(a) is an inherent characteristic of DPIV measurements of a vortex using a rectangular array and is due to quantization. Figure 2(b) shows the rotating wave, with a dominant mode  $k=4$  at  $Re=2500$ . The flow in the inner region remains essentially axisymmetric, indicating that the breaking of symmetry to azimuthal mode  $k=4$  originates from the instability of the jet-like shear layer pumping vorticity up from the boundary layer on the rotating floor by the stationary cylinder. A similar behavior was recently observed in three-dimensional computations for the case of a stationary rigid top.<sup>4</sup> The data shown in Fig. 2(b) were obtained by phase-averaging the DPIV measurements at each 1/4 rotation of the wave over a period of 100 s in order to reduce the random DPIV noise.

Figure 3 gives four instantaneous measurements (not phase averaged) of the rotating wave state at  $Re=2500$  showing the retrograde (with respect to the floor rotation) precession of the wave. Although there is considerable noise in the data [as compared to phase-locked data in Fig. 2(b)], particularly the vorticity which is computed from the velocity data obtained via DPIV, the mode  $k=4$  wave in the outer region of the flow is clearly identifiable. The sequence of snapshots in the figure are at times  $0.0625T_{RW}$  apart, where  $T_{RW}$  is the precession period of the wave. The time required for the wave to spontaneously develop and grow is relatively long, of order  $10^3$  rotations of the floor. This is consistent with its onset being via a supercritical Hopf bifurcation, where the growth rate near onset is close to zero.

Figure 4 shows how the amplitude and (precession) period of the rotating wave vary with  $Re$ . As a measure of the amplitude, we use the area integral of the perturbation axial vorticity squared,  $\omega_p^2$ . The area integration was performed only up to approximately  $0.87R$  in order to minimize error

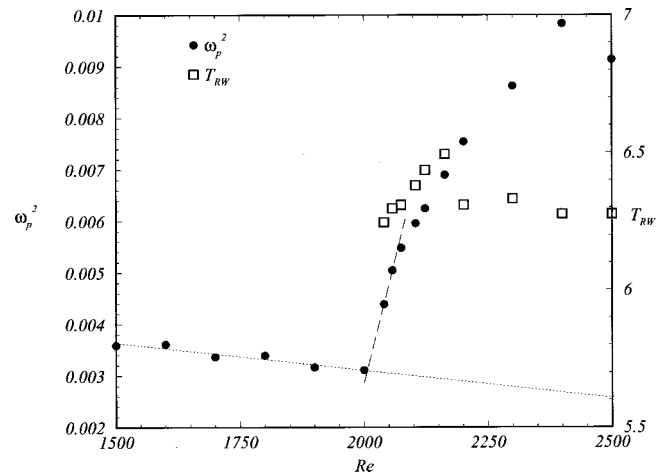


FIG. 4. Disturbance amplitude at  $z=0.76H$ , defined as the area integral of the perturbation vorticity squared,  $\omega_p^2$  (nondimensionalized with  $\Omega$ ), and the precession period of the rotating wave,  $T_{RW}$  (nondimensionalized with the floor rotation period), as functions of  $Re$ .

due to DPIV noise near the wall. The perturbation axial vorticity is determined by subtracting the azimuthally averaged axial vorticity from the local axial vorticity, and is nondimensionalized by  $\Omega$ . Due to the Cartesian nature of the vorticity measurements, obtained from DPIV, the data had to be transformed into polar coordinates prior to averaging in the azimuthal direction. The algorithm for transforming the Cartesian data into polar coordinates involved a single parameter,  $N$ , giving the number of points in the Cartesian data set that are interpolated into a discrete annular grid. The data shown used  $N=36$ . We have found that varying  $N$  from 4 to 64 changes the magnitude of  $\omega_p^2$  by less than  $\pm 10\%$ .<sup>15</sup> However, the extrapolated value of  $Re$  for the supercritical Hopf bifurcation (approximately 2000), corresponding to the intersection of the linear growth line and the base DPIV noise level, was found to be independent of  $N$  for the range of values considered. The linear growth from (essentially) zero of the perturbation axial vorticity squared with  $Re$  from the onset of the wave, together with the precession period being finite and only varying slowly with  $Re$  from the onset, are characteristics of a supercritical Hopf bifurcation breaking  $SO(2)$  symmetry. The precession period,  $T_{RW}$  (nondimensionalized by the rotation of the floor,  $2\pi/\Omega$ ), varies by less than 10% over a wide range of  $Re$  from the onset of symmetry breaking. The nonlinear saturation of  $\omega_p^2$  is also apparent in the figure.

Previous axisymmetric computations<sup>11,13</sup> have determined that the basic state undergoes a supercritical axisymmetric Hopf bifurcation at  $Re > 2500$ , i.e., at much larger  $Re$  than the symmetry breaking Hopf bifurcation to a rotating wave reported here. Our observations are consistent with the flow visualization experiments of Ref. 9 which report instability at  $Re \sim 2000$ , but they do not detail the nature of the instability nor its physical origin. From our DPIV measurements of the velocity and determined vorticity, it is apparent that the symmetry breaking is due to an azimuthal instability of the shear layer that is produced by the turning of the boundary layer on the rotating disk into the interior, and that the central recirculation zone plays no role in this instability.

The experiments of Ref. 8 report two period doublings as  $Re$  is increased beyond 2000 from spectra obtained using a single point laser Doppler velocimeter system, although they do not report on the spatial structure of the instabilities. In light of our present data, we conjecture that their period doublings correspond to precession periods of azimuthal modes  $k=4$ , 2, and 1 successively. With the inherent noise level in the instantaneous DPIV data, i.e., nonphase averaged, we are presently unable to unambiguously identify the possible secondary bifurcations leading to period doublings from  $k=4$  to  $k=2$  and then to  $k=1$  (each of these secondary bifurcated states would still have large  $k=4$  components and very weak  $k=2$  and  $k=1$  components). We are currently investigating this possible scenario with full three-dimensional computations, along the lines of the study in Ref. 6.

### ACKNOWLEDGMENTS

We wish to thank Michael J. Vogel for his assistance in many aspects of the DPIV measurements and data analysis. This work was supported by NSF Grants No. CTS-0116947 and No. CTS-0116995.

<sup>1</sup>H. M. Blackburn and J. M. Lopez, "Symmetry breaking of the flow in a cylinder driven by a rotating endwall," *Phys. Fluids* **12**, 2698 (2000).

<sup>2</sup>H. M. Blackburn and J. M. Lopez, "Modulated rotating waves in an enclosed swirling flow," *J. Fluid Mech.* (to be published).

<sup>3</sup>A. Y. Gelfgat, P. Z. Bar-Yoseph, and A. Solan, "Three-dimensional insta-

bility of axisymmetric flow in a rotating lid-cylinder enclosure," *J. Fluid Mech.* **438**, 363 (2001).

<sup>4</sup>F. Marques and J. M. Lopez, "Precessing vortex breakdown mode in an enclosed cylinder," *Phys. Fluids* **13**, 1679 (2001).

<sup>5</sup>F. Marques, J. M. Lopez, and J. Shen, "Mode interactions in an enclosed swirling flow: A double Hopf bifurcation between azimuthal wavenumbers 0 and 2," *J. Fluid Mech.* **455**, 263 (2002).

<sup>6</sup>J. M. Lopez, J. E. Hart, F. Marques, S. Kittelman, and J. Shen, "Instability and mode interactions in a differentially-driven rotating cylinder," *J. Fluid Mech.* (to be published).

<sup>7</sup>A. Spohn, M. Mory, and E. J. Hopfinger, "Observations of vortex breakdown in an open cylindrical container with a rotating bottom," *Exp. Fluids* **14**, 70 (1993).

<sup>8</sup>D. L. Young, H. J. Sheen, and T. Y. Hwu, "Period-doubling route to chaos for a swirling flow in an open cylindrical container with a rotating-disk," *Exp. Fluids* **18**, 389 (1995).

<sup>9</sup>A. Spohn, M. Mory, and E. J. Hopfinger, "Experiments on vortex breakdown in a confined flow generated by a rotating disk," *J. Fluid Mech.* **370**, 73 (1998).

<sup>10</sup>D. T. Valentine and C. C. Jahnke, "Flows induced in a cylinder with both end walls rotating," *Phys. Fluids* **6**, 2702 (1994).

<sup>11</sup>J. M. Lopez, "Unsteady swirling flow in an enclosed cylinder with reflectional symmetry," *Phys. Fluids* **7**, 2700 (1995).

<sup>12</sup>J. M. Lopez and J. Chen, "Coupling between a viscoelastic gas/liquid interface and a swirling vortex flow," *J. Fluids Eng.* **120**, 655 (1998).

<sup>13</sup>M. Brons, L. K. Voigt, and J. N. Sorensen, "Topology of vortex breakdown bubbles in a cylinder with a rotating bottom and a free surface," *J. Fluid Mech.* **428**, 133 (2001).

<sup>14</sup>A. H. Hirsa, J. M. Lopez, and R. Miraghaie, "Measurement and computation of hydrodynamic coupling at an air/water interface in the presence of an insoluble monolayer," *J. Fluid Mech.* **443**, 271 (2001).

<sup>15</sup>R. Miraghaie, Ph.D. thesis, Rensselaer Polytechnic University, 2002.